Linkage of Multiequilibria in DNA Recognition by the D53H *Escherichia coli* cAMP Receptor Protein†

Shwu-Hwa Lin and J. Ching. Lee*

Department of Human Biological Chemistry and Genetics, The University of Texas Medical Branch at Galveston, Galveston, Texas 77555-1055

Received August 29, 2002; Revised Manuscript Received October 22, 2002

ABSTRACT: The transcription factor cyclic AMP receptor protein, CRP, regulates the operons that encode proteins involved in translocation and metabolism of carbohydrates in *Escherichia coli*. The structure of the CRP−cAMP complex reveals the presence of two sets of cAMP binding sites. Solution biophysical studies show that there are two high-affinity and two low-affinity binding sites, to which the binding of cAMP is characterized by varying degrees of cooperativity. A stoichiometry of four implies that potentially CRP can exist in five conformers with different numbers of bound cAMP. These conformers may exhibit differential affinities for specific DNA sequences. In this study, the affinity between DNA and each conformer of D53H CRP was defined through a dissection of the thermodynamic linkage scheme that included all the conformers. Loading of the high- and low-affinity sites with cAMP leads to high and low affinity for DNA, respectively. The specific magnitude of the binding constants of these conformers is DNA sequence dependent. The various association constants defined by the present study provide a solution to address an enigma of the CRP system, namely, the 3 orders of magnitude difference between the cAMP binding constants determined by in vitro studies and the cAMP concentration regime to which the bacteria respond. Under physiological conditions, the apo-CRP−DNA complex is the dominant species. As a consequence of the 1000-fold stronger affinity of cAMP to the apo-CRP−DNA complex than that to CRP, the relevant reaction is the binding of cAMP to this DNA−protein complex. The binding constant is of the order of 10^7 M^{-1}, the same concentration regime as that of cellular concentration of cAMP. In addition, under physiological conditions the species that binds to the *lac* and *gal* operons is predicted to be CRP−$(cAMP)_1$. A comparison of parameters between the wild type and the mutant CRP shows that the mutation apparently shifts the various thermodynamically linked equilibria without a change in the basic mechanism that governs CRP activities. Thus, the conclusions derived from a study of the mutant are relevant to wild-type CRP. A dissection of the individual binding constants in this multiequilibria reaction scheme leads to a definition of the mechanism of action of this transcription factor.

The binding of cAMP receptor protein (CRP)[1] to the operons activates the transcription of over 20 different operons encoding proteins involved in translocation and metabolism of carbohydrates in *Escherichia coli*. CRP is a dimer of two identical subunits, each consisting of 209 amino acids (*1*, *2*). The crystal structure of the CRP−cAMP complex shows that each subunit is folded into two distinct functional and structural domains. They are connected by a hinge region (residues 130−138). The large N-terminal domain contains a long C-helix that is essential for subunit−subunit contact and an extensive network of β-sheets forming the cAMP-binding pocket. The small C-terminal domain consists of the DNA binding helix−turn−helix motif that makes base-specific contacts with CRP-dependent promoters (*3*).

One key issue that yet has to be resolved is the mechanism of the allosteric activation of CRP by cAMP binding. Biochemical and biophysical evidences show that binding of cAMP allosterically induces CRP to assume a conformation that exhibits a high affinity for a specific DNA sequence (*4*−*13*). Detailed secondary and tertiary structural information of the CRP−$(cAMP)_2$ and the DNA−CRP−$(cAMP)_2$ cocrystal complexes is available (*3*, *14*, *15*). On the basis of these structural data, the currently favored model for the allosteric activation of CRP by cAMP involves subtle changes in the CRP structure such as a rolling change in the relative positions of the C-helices leading to a rigid body motion of the domains with respect to each other (*16*). Several lines of evidence suggest that transmission of information may involve the interfacial interactions between domains and subunits (*17*−*20*). For example, correlation between a weak affinity for subunit assembly and the relaxation of cNMP selectivity in the G141Q and S128A/G141Q mutants suggests that intersubunit interaction is important for cyclic nucleotide discrimination in CRP (*19*).

† Supported by NIH Grant GM45579 and Robert A. Welch Foundation Grants H-0013 and H-1238.

* Author to whom correspondence should be addressed. Tel: (409) 772-2281; fax: (409) 772-4298; e-mail: jclee@utmb.edu.

[1] Abbreviations: cAMP, 3′,5′-cyclic adenosine monophosphate; cGMP, 3′,5′-cyclic guanosine monophosphate; cNMP, 3′,5′-cyclic nucleotide monophosphate; WT, wild type; CRP, cAMP receptor protein; CPM, *N*-[4-[7-(diethylamino)-4-methylcoumarin-3-yl]phenyl]-maleimide; TEK(100), 50 mM Tris, 100 mM KCl, 1 mM EDTA at pH 7.8 and 25 °C; PAGE, polyacrylamide gel electrophoresis.

10.1021/bi026756n CCC: $22.00
Published on Web 11/21/2002

Recently, this correlation was extended by the results of a study of WT and eight CRP mutants (*21*). In addition, in the absence of cAMP, mutant G141Q was sensitive to protease attack at the subunit interface, an established property of WT CRP observed only in the presence of cAMP. This observation implies that the G141Q mutant exhibits a subunit alignment similar to that of the activated CRP (*18*). Furthermore, chemical modification of the C-terminal DNA binding domain of the G141Q mutant showed that the DNA binding domain responds quantitatively to the binding of cyclic nucleotide to the N-terminal domain. This result suggests the involvement of a long-range communication between domains (*18*).

Although the literature seems to favor the concept of a specific pathway of signal transmission, these observations are consistent with an alternative interpretation. Instead of transmitting via a specific pathway that involves breaking and forming of specific bonds, CRP is a molecule that is in dynamic motions more appropriately represented by an ensemble of microstates. The activation process represents a shifting of the distribution of these microstates toward the ensemble of active states. Recent studies from this laboratory have shown that this global conformational switch involves a change in structural dynamics that is manifested in subunit realignment and domain rearrangement (*17*−*19*, *21*−*24*). Solution thermodynamic and structural studies indicate that the message imparted by cAMP binding is sensed by many remote parts of the molecule in a global manner (*25*). The strongest supportive evidence for this global effect is the ability to obtain an identical binding constant for cAMP to WT CRP using signals generated from different parts of CRP (*25*).

In search of a structure of CRP in its allosterically activated form, molecular genetic studies were conducted to identify a novel class of mutation in the *crp* gene, CRP*, which does not require exogenous cAMP for activation (*26*, *27*). Most of the mutations, which lead to the CRP* phenotype, are located either in the hinge region between the cAMP and the DNA binding domain or in the region that is assumed to be involved in cAMP binding (*28*). It was hypothesized that the amino acid substitutions alter the allosteric nature of CRP and thereby allow the protein to act in the absence of cAMP. In a recent biophysical study involving a number of these CRP* mutants, it became clear that these mutations do not alter the basic mechanism of CRP activation. These mutations more likely function by perturbing the various thermodynamically linked reactions (*21*).

To resolve the issue of whether there is a specific allosteric pathway through which signal is transmitted or if the mechanism is more appropriately represented by a shifting of an ensemble of microstates, it is useful to compare and contrast the linked reactions carried out by these CRP* mutants and WT CRP. In this study, the D53H CRP mutant, which displays a CRP* phenotype, is the subject of investigation. Could D53H CRP bind specific sequence of DNA in the absence of cAMP or in the presence of cGMP, in vitro? D53H mutation enhances the extent of cooperativity of cAMP binding. This result implies that there is an increase in subunit−subunit communication (*22*). Since residue 53 is not directly involved in cAMP binding, in subunit−subunit interaction, or in DNA binding, how does a mutation at this site affect the protein property and function? Does D53H CRP function through an altered pathway of intermolecular communication? D53H CRP apparently exhibits properties that make it a very attractive target for studying the activation mechanism of CRP.

EXPERIMENTAL PROCEDURES

Materials

cAMP and cGMP were purchased from Sigma (Saint Louis, MO). CPM was purchased from Molecular Probes Inc. (Eugene, OR). Oligonucleotides were synthesized by Genosys (Woodlands, TX). Bactotryptone and yeast extract were obtained from Difco Laboratories (Detroit, MI). All other reagents were the highest grade commercially available.

Methods

All experiments, except specifically indicated, were conducted in buffer TEK(100). The concentrations of protein, cyclic nucleotides, and fluorescence probe were determined by absorption spectroscopy using the following absorption coefficients: 40 800 M^{-1} cm^{-1} at 278 nm for CRP dimer (*29*); 14 650 M^{-1} cm^{-1} at 259 nm and 12 950 M^{-1} cm^{-1} at 254 nm for cAMP and cGMP (*30*), respectively; and 33 000 M^{-1} cm^{-1} at 385 nm for CPM.

Protein Purification. The WT and D53H CRPs were prepared from a well-established expression system as previously described (*22*, *25*). Proteins were isolated and purified by sequential chromatography on Bio-Rex 70, hydroxyapatite (Bio-Rad), and phenyl Sepharose (Amersham Pharmacia Biotech, Uppsala, Sweden). Purified proteins are >99% homogeneous as routinely analyzed with SDS−PAGE stained by Coomassie Blue with a loading of 50−60 μg/lane. DNA contamination was judged to be negligible since the ratio of the absorbance at 280 nm to that at 260 nm was larger than 1.86. Proteins were stored in the buffer containing 50 mM phosphate, 1 mM EDTA, 1 mM DTT, 100 mM KCl, and 10% glycerol at pH 7.5 and −20 °C. Before being used for experimentations, CRPs were routinely dialyzed against the described buffer and then gently filtered through a membrane with a pore size of 0.22 μm.

Labeling of DNA with Fluorescent Probe. Details for CPM-labeled double-stranded DNA preparation were previously described (*31*, *32*). Briefly, single-stranded DNA was purified by 15% acrylamide PAGE, in the presence of 7.5 M urea. EDC (1-ethyl-3,3-dimethylaminopropylcarbodiimide) coupling with cystamine to purified phosphorylated oligomer was used to conduct thiol modification at the single-stranded DNA. Subsequently, covalent attachment of CPM to the thiol-modified single-stranded DNA was performed. Each oligomer was then hybridized to its complementary strand. The integrity of the oligomers was monitored by PAGE under nondenaturing conditions. Contamination of CPM-labeled single-stranded DNA was judged to be negligible if only a single band was observed on PAGE illuminated with UV light. Finally, CPM-labeled DNA samples were dialyzed against buffer containing 50 mM Tris and 1 mM EDTA at pH 7.8 and stored at −20 °C. DNA sequences used in the current study are *lac26*, *gal26*, *lac40*, and *nonspecific26* with the sequence 5′-ATTAATGTGAGTTAGCTCACTCATTA-3′, 5′-AAAAGTGTGACATGGAATAAATTAGT-3′, 5′-GCAACGCAATTAATGTGAGT-

Scheme 1

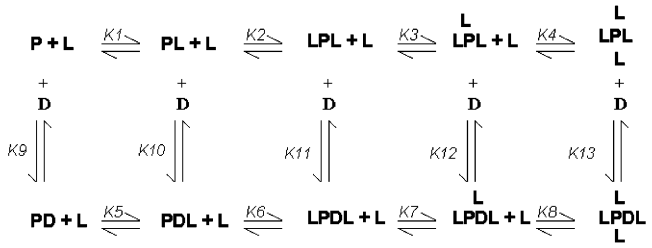

TAGCTCACTCATTA-GGCACCC-3′, and 5′-CTCAGT-TCTGA-TACCAAGCAGCCCAG-3′, respectively. The underlined sequences are the primary binding sites for CRP.

DNA Binding Study. Fluorescence anisotropy experiment was employed for measurements of the CRP−DNA interaction (*31*, *32*). Solutions containing *lac26*−CPM (12 nM) or *gal26*−CRP (14.6 nM) and cAMP (from 0 to 85 mM) were titrated with D53H CRP. A description on the binding of CRP to DNA was published previously (*33*). Briefly, the measured anisotropy data of the CRP−DNA interaction were analyzed according to the following equation:

$$A_{obs} = A_0 + \Delta A\frac{K_{app}(D_T + P_T) + 1 - \sqrt{(K_{app}(D_T + P_T) + 1)^2 - 4K_{app}^2 D_T P_T}}{2K_{app}D_T} \quad (1)$$

to estimate the apparent association constant (K_{app}) for the binding of CRP to DNA at a fixed cAMP concentration. A_{obs}, A_0, ΔA, P_T, and D_T are the observed anisotropy, anisotropy of free DNA, total change in anisotropy, and total protein and DNA concentration, respectively. Dilution of the solutions during the titration affected the fitted parameters. Therefore, the effect of dilution of DNA was taken into consideration during data analysis. The fitted parameters with standard deviations were obtained by nonlinear curve fitting with the Marquardt−Levenber algorithm provided by Sigmaplot version 5.0.

Mechanism of CRP−cAMP−DNA Tertiary Complex Formation. CRP possesses four cAMP binding sites and thus potentially exhibits five conformers, P, PL, PL_2, PL_3, and PL_4. A detailed description of DNA binding to various species of CRP is shown in Scheme 1. The first two cAMP binding sites exhibit constants that are about 2 orders of magnitude higher than the second set of two (*22*). Thus, the four cAMP binding sites in CRP can be treated as two sets of sites. In Scheme 1, P, D, and L are protein, DNA, and cAMP, respectively.

K_1, K_2, K_3, and K_4 are the association constants of the loading of the first, second, third, and fourth cAMP site of CRP by ligand; therefore, $K_1 = [PL]/[P][L]$, $K_2 = [PL_2]/[PL][L]$, $K_3 = [PL_3]/[PL_2][L]$, and $K_4 = [PL_4]/[PL_3][L]$. The relationship between K_1, K_2, K_3, and K_4 and the microscopic association constants of cAMP binding to CRP are $K_1 = 2k_1^1$, $K_2 = 1/2k_1^2$, $K_3 = 2k_2^1$, and $K_4 = 1/2k_2^2$. These parameters were defined in a previous study (*22*). k_1^1 and k_1^2 are the binding constants for the first and second ligand to the two strong sites, respectively. k_2^1 and k_2^2 are the equivalent parameters to the weak sites. K_5, K_6, K_7, and K_8 are the association constants of the loading of the first, second, third, and fourth cAMP site of a CRP−DNA complex by ligand; therefore, $K_5 = [DPL]/[DP][L]$, $K_6 = [DPL_2]/[DPL][L]$, $K_7 = [DPL_3]/[DPL_2][L]$, and $K_8 = [DPL_4]/[DPL_3][L]$. K_9, K_{10}, K_{11}, K_{12}, and K_{13} are the association constants for the formation of CRP−DNA complexes, PD, PDL, PDL_2, PDL_3, and PDL_4, respectively. Thus, $K_9 = [DP]/[P][D]$, $K_{10} = [DPL]/[PL][D]$, $K_{11} = [DPL_2]/[PL_2][D]$, $K_{12} = [DPL_3]/[PL_3][D]$, and $K_{13} = [DPL_4]/[PL_4][D]$. K_5, K_6, K_7, and K_8 can be calculated from the relationships of $K_5 = K_1K_{10}/K_9$, $K_6 = K_2K_{11}/K_{10}$, $K_7 = K_3K_{12}/K_{11}$, and $K_8 = K_4K_{13}/K_{12}$.

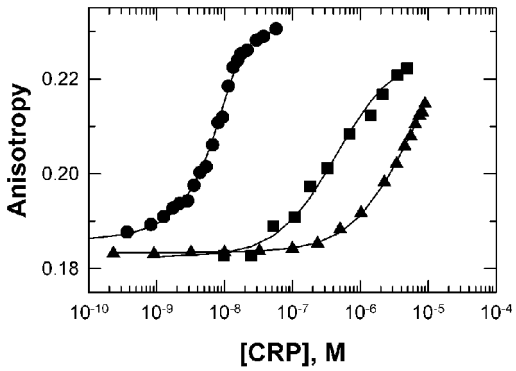

FIGURE 1: Binding isotherms for D53H CRP to *lac26*−CPM DNA in the presence of 200 μM cAMP (●) and 200 μM cGMP (▲) or in the absence of cNMP (■) as monitored by fluorescence anisotropy. The solid lines represent the best fit according to eq 1 in Methods. The fitting results are listed in Table 1.

Table 1: Apparent DNA Binding Affinity of the WT and D53H CRP

DNA	ligand[a]	K_{app} ($\times 10^6$ M^{-1}) WT	D53H
lac26	cAMP	50 ± 6	730 ± 120
	cGMP	<0.05	0.19 ± 0.01
	none	<0.01	2.3 ± 0.4
gal26	cAMP	12 ± 0.8	216 ± 11
	none	<0.05	0.65 ± 0.07[b]
nonspecific	cAMP	0.05[c]	0.51 ± 0.06
	none	nm[d]	<0.04[b]

[a] When cNMP was present, the concentration was 200 μM. [b] Fitted under the constraint that $\Delta A = 0.065$ (eq 1). [c] Data from ref *31*. [d] No measurable affinity under the experimental condition.

RESULTS

DNA Binding Isotherms. In vivo study shows that D53H CRP exhibits CRP* phenotypic behavior (*28*), implying that D53H CRP is able to bind to specific DNA sites either in the absence of exogenous cAMP or in the presence of cGMP. However, an earlier in vitro study of another CRP* mutant, G141Q, showed that it requires cNMP binding for allosteric activation (*34*). Hence, an in vitro DNA binding study for D53H CRP was initiated. As shown in Figure 1, D53H CRP binds to *lac26* either in the presence of cAMP or cGMP and binds to DNA with significant affinity even in the absence of cNMP. The apparent equilibrium constant for the complex formation between D53H and *lac26* was 7.3×10^8 M^{-1} in the presence of 200 μM cAMP. This result reflects an apparent 15-fold enhancement in DNA binding affinity as compared to that of WT CRP (Table 1).

lac26 DNA Binding Affinity of D53H CRP Conformers. Since CRP potentially exists in five conformers, P, PL, PL_2,

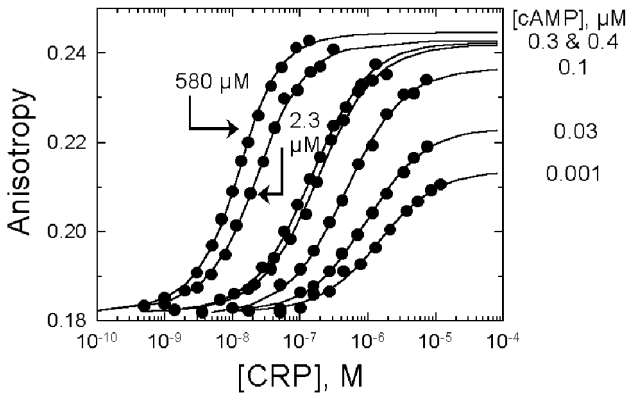

FIGURE 2: Typical binding isotherms for D53H CRP to DNA as a function of cAMP concentration. Titrations were performed with 14.6 nM *lac26*−CPM and with indicated cAMP concentrations. The anisotropy of CRP-labeled *lac26* DNA was normalized to 0.1800. Solid lines represent the best fit of eq 1 to the observed data.

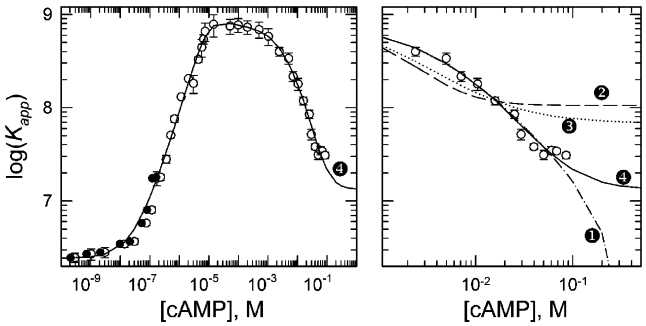

FIGURE 3: cAMP concentration dependence of the apparent association constant (K_{app}) for D53H CRP binding to *lac26*. Error bars indicated the uncertainty in K_{app} estimated at each cAMP concentration. The data were analyzed according to eq 2, and the best fit is shown by the sold line (left panel). The lines identified by numbered solid circles in the right panel represent the best fit of the cAMP dependence of the affinity for D53H CRP binding to *lac26* under different constraints, as described in the corresponding cases in Table 2, which also lists the recovered parameters.

PL_3, and PL_4, the apparent equilibrium constant at a fixed cAMP concentration is a composite of several equilibria and reflects the affinity of the various CRP conformers for the DNA sequence. A series of titration experiments conducted at different cAMP concentrations, as shown in Figure 1, can provide information on the dependence of K_{app} on cAMP concentration. This information allows a dissection of the affinity between DNA and each CRP conformer, as shown by Heyduk and Lee (*32*). A representative set of DNA binding isotherms as a function of cAMP concentration is shown in Figure 2. The value of K_{app} for each isotherm was determined by fitting the data to eq 1. Since K_{app} is sensitive to ionic strength of the buffer and to exclude this effect in K_{app} measurement, a varying concentration of KCl was employed to keep the total salt concentration equal to 100 mM when [cAMP] > 1 mM. Figure 3 shows the dependence of the apparent equilibrium constants for D53H−*lac26* complexes as defined by 37 binding isotherms in varying concentrations of cAMP. The data are represented by a bell-shape curve. The apparent equilibrium constant increases with increasing cAMP concentration, reaches a plateau value, and then decreases at very high cAMP concentration. According to Scheme 1, the cAMP concentration dependence of the apparent equilibrium constants for D53H−DNA complex formation can be expressed as follows:

$$K_{app} = \frac{K_9 + K_1K_{10}[L] + K_1K_2K_{11}[L]^2 + K_1K_2K_3K_{12}[L]^3 + K_1K_2K_3K_4K_{13}[L]^4}{1 + K_1[L] + K_1K_2[L]^2 + K_1K_2K_3[L]^3 + K_1K_2K_3K_4[L]^4} \quad (2)$$

In Scheme 1, there are 13 parameters to describe the reaction of DNA binding to CRP linked to the cAMP binding reactions. The number of fitting parameters could be reduced by providing information on the binding affinity between cAMP and each CRP conformer determined by an independent measurement. In an earlier study, the association constants governing the interaction of cAMP with CRP were determined by calorimetry and fluorescence titration (*22*). The various equilibrium constants are as follows: $K_1 = 2k_1^1 = 4 \times 10^4\ M^{-1}$, $K_2 = 1/2k_1^2 = 3 \times 10^5\ M^{-1}$, $K_3 = 2k_2^1 = 9 \times 10^2\ M^{-1}$, and $K_4 = 1/2k_2^2 \approx 0$. Furthermore, in this study K_9 was determined directly in the absence of cAMP, as shown in Figure 1. The experimentally observed value is $2.4 \times 10^6\ M^{-1}$ for K_9. Since K_5, K_6, K_7, and K_8 can be calculated, in accordance to the thermodynamic linkage relationships, only the values of the remaining four DNA binding association constants, K_{10}, K_{11}, K_{12}, and K_{13}, have to be determined. In practice, determination of K_{10}, K_{11}, K_{12}, and K_{13} can be achieved through nonlinear least-squares fitting of the experimentally obtained individual K_{app} as a function of cAMP concentration. It is expected that the uncertainty of recovered K_{13} and K_{14} would be relatively large because of limited information of K_{app} at high cAMP concentrations and imprecise determination of the cAMP association constants for the low-affinity cAMP binding sites, k_2^1 and k_2^2 (*22*). Therefore, data analysis was conducted under various constraints with different assumptions. The criteria for acceptable solution for the fitted parameters are that the recovered parameters should be consistent with cAMP binding parameters determined independently such as those reported by Lin and Lee (*22*) and physically relevant, such as assuming a positive value. The recovered parameters with standard errors were obtained by fitting eq 2 to the observed data with the Marquardt−Levenber algorithm provided by Sigmaplot version 5.0. The goodness of the fit was judged by the values of adjusted R^2 and Durbin−Watson statistic. When the value of the adjusted R^2 approached 1, it indicated that the equation was a good description of the relation between the independent and the dependent variables. However, the tested model was rejected if the Durbin−Watson value deviated from 2 by more than 0.5 (i.e., below 1.5 or above 2.5), suggesting correlated residuals.

Case 1: Two Identical, Independent Low-Affinity cAMP Binding Sites. Each CRP conformer binds *lac26* with different affinity. Constraints: $K_4 = 1/4K_3 = 2k_2^1$ and $K_{10} \neq K_{11}$, $K_{12} \neq K_{13}$. Although it was difficult to precisely define k_2^1 and k_2^2 (therefore, K_3 and K_4) in the cAMP binding study, a limit for the association constant for cAMP bound to the low-affinity site was set as $K_3 = 920\ M^{-1}$ (*22*). By assuming that the two low-affinity cAMP binding sites are identical and independent, the values of the association constant for various CRP conformers bound to *lac26* (K_{10}, K_{11}, K_{12}, and K_{13}) were estimated from fitting eq 2 to the observed data

Table 2: Recovered Parameters from the *lac26*−D53H CRP Interaction

case	constraints[a]	line	recovered parameters	calculated parameters[b]	
1	$K_3 = 2k^1_2 = 920\ M^{-1}$ $K_4 = 1/2k^2_2 = 230\ M^{-1}$	①	$K_{10} = (2.1 \pm 0.1) \times 10^9\ M^{-1}$ $K_{11} = (7.5 \pm 0.2) \times 10^8\ M^{-1}$ $K_{12} = (5.5 \pm 0.4) \times 10^8\ M^{-1}$ $K_{13} = (-7 \pm 14) \times 10^6\ M^{-1}$	$K_5 = 3.5 \times 10^7\ M^{-1}$ $K_6 = 9.7 \times 10^4\ M^{-1}$ $K_7 = 6.7 \times 10^3\ M^{-1}$ $K_8 =$ ND[e]	$R^2 = 0.988$[c] DW = 1.634[d]
2	$K_3 = 2k^1_2 = 920\ M^{-1}$ $K_4 = 1/2k^2_2 = 230\ M^{-1}$ $K_{12} = K_{13}$	②	$K_{10} = (1.8 \pm 0.2) \times 10^9\ M^{-1}$ $K_{11} = (8.7 \pm 0.4) \times 10^8\ M^{-1}$ $K_{12} = (1.1 \pm 0.2) \times 10^8\ M^{-1}$	$K_5 = 3.0 \times 10^7\ M^{-1}$ $K_6 = 1.3 \times 10^5\ M^{-1}$ $K_7 = 110\ M^{-1}$ $K_8 = 200\ M^{-1}$	$R^2 = 0.945$ DW = 0.55
3	$K_3 = 2k^1_2 = 920\ M^{-1}$ $K_4 = 0$ $K_{13} = 0$	③	$K_{10} = (1.8 \pm 0.2) \times 10^9\ M^{-1}$ $K_{11} = (8.7 \pm 0.3) \times 10^8\ M^{-1}$ $K_{12} = (7 \pm 2) \times 10^7\ M^{-1}$	$K_5 = 3.0 \times 10^7\ M^{-1}$ $K_6 = 1.3 \times 10^5\ M^{-1}$ $K_7 = 8.6\ M^{-1}$	$R^2 = 0.963$ DW = 0.75
4	$K_4 = n^*K_3$ $K_{13} = K_{12}$	④	$K_3 = 290 \pm 50\ M^{-1}$ $n = 0.069 \pm 0.15$ $K_{10} = (2.1 \pm 0.1) \times 10^9\ M^{-1}$ $K_{11} = (7.5 \pm 0.2) \times 10^8\ M^{-1}$ $K_{12} = (1 \pm 2) \times 10^7\ M^{-1}$	$K_5 = 3.5 \times 10^7\ M^{-1}$ $K_6 = 9.7 \times 10^4\ M^{-1}$ $K_7 = 5\ M^{-1}$ $K_8 = 20\ M^{-1}$	$R^2 = 0.988$ DW = 1.65

[a] $K_1 = 2k^1_1 = 4 \times 10^4\ M^{-1}$, $K_2 = 1/2k^2_1 = 3 \times 10^5\ M^{-1}$ (*22*), and $K_9 = 2.4 \times 10^6\ M^{-1}$. [b] $K_5 = K_1K_{10}/K_9$, $K_6 = K_2K_{11}/K_{10}$, $K_7 = K_3K_{12}/K_{11}$, and $K_8 = K_4K_{13}/K_{12}$. [c] Adjusted R^2. [d] Durbin−Watson statistic. [e] Not determined.

with constraints of $K_3 = 2k^1_2 = 920\ M^{-1}$ and $K_4 = 1/2k^2_2 = 230\ M^{-1}$. A negative value was returned for K_{13}, and the result of the fit is shown in the right panel of Figure 3, line ①. A negative value for any fitted parameter indicates physical irrelevance. Thus, case 1 does not seem to be a viable model to represent the data. Furthermore, the fitted curve deviated from the data at high cAMP concentration. The value for the observed K_{app} at very high cAMP concentration approached a constant finite value but not to 0, as shown in Figure 3. However, the fitted curve approached zero. Thus, this model was rejected since it could not fit the observed data at very high cAMP concentrations.

Case 2: Two Identical, Independent Low-Affinity cAMP Binding Sites. PL_3 and PL_4 have identical affinity for *lac26*. Constraints: $K_4 = 1/4K_3 = 2k^1_2$ and $K_{12} = K_{13}$. Line ② in the right panel of Figure 3 represents the best fit of eq 2 to the observed data yielding values of $K_{10} = (1.8 \pm 0.2) \times 10^9\ M^{-1}$, $K_{11} = (8.7 \pm 0.4) \times 10^8\ M^{-1}$, and $K_{12} = (1.1 \pm 0.2) \times 10^8\ M^{-1}$. Again, the curve does not fit the data at high concentrations of cAMP. Additionally, the Durbin−Watson statistic was as low as 0.55, and thus this model was rejected.

Case 3: Strong Negative Cooperativity between the Two Low-Affinity cAMP Binding Sites. Constraints: $K_3 = 920\ M^{-1}$, $K_4 = 0$ and $K_{13} = 0$. The difficulty in defining K_4 in the cAMP binding study by Lin and Lee (*22*) implies that either the conformer PL_4 does not exist, or the affinity is too weak to be detected within these experimental conditions. Thus, in this analysis, K_4 and K_{13} were assumed to equal 0. Line ③ in Figure 3, right panel, represents the best fit under these constraints and the fit resulted in $K_{10} = (1.8 \pm 0.2) \times 10^9\ M^{-1}$, $K_{11} = (8.7 \pm 0.3) \times 10^8\ M^{-1}$, and $K_{12} = (6.8 \pm 1.7) \times 10^7\ M^{-1}$. The deviation of the fitted curve from experimental data at high concentrations of cAMP suggested that K_4 and K_{13} are necessary parameters to describe the overall reaction.

Case 4: Identical but Interacting Low-Affinity cAMP Binding Sites. Constraints: $K_{12} = K_{13}$ and $K_4 = nK_3$. The best fitting result is shown as line ④, with the values of $K_3 = 290 \pm 50\ M^{-1}$, $n = 0.069 \pm 0.15$, $K_{10} = (2.1 \pm 0.1) \times 10^9\ M^{-1}$, $K_{11} = (7.5 \pm 0.2) \times 10^8\ M^{-1}$, and $K_{12} = (1.3 \pm 2.1) \times 10^7\ M^{-1}$. The value of K_3 is consistent with the result obtained from the cAMP binding study (*22*). The large error for the estimation of n is expected because of the limited amount of information available at high cAMP concentrations. However, the value of n still provides very important information. The ratio of $K_4/K_3 = n = 0.069 \pm 0.15 < 0.25$ suggests that there is negative cooperativity between the two low-affinity sites, a conclusion similar to that derived from the cAMP binding study (*22*). In all cases, the fitted parameters of K_{10} and K_{11} are essentially identical regardless of the constraints employed in the analysis, namely, $K_{10} \sim 2 \times 10^9\ M^{-1} > K_{11} \sim 8 \times 10^8\ M^{-1}$. Furthermore, the relative order of affinity is consistent in all cases, namely, $K_{10} > K_{11} > K_{12}$.

According to eq 2, data analysis for DNA binding and its cAMP dependence required an assumption that the free cAMP concentration equals to the total cAMP concentration. However, this assumption was not valid in the cAMP concentration ranging from 0 to 1×10^{-6} M. It is necessary to examine whether the error in the determination of cAMP concentration affects the results in data analysis. On the basis of the values of $K_1 = 4 \times 10^4\ M^{-1}$, $K_2 = 3 \times 10^5\ M^{-1}$, and $K_6 = 9.7 \times 10^4\ M^{-1}$, the complexes of PL, PL_2, and PDL_2 would appear in solution only when [cAMP] $> 5 \times 10^{-6}$ M. Thus, one can estimate that approximately 70−90% of total cAMP was free in solution, based on a 10 nM DNA−CRP complex, $K_5 = 3.5 \times 10^7\ M^{-1}$, and a total cAMP concentration in the range of ∼1−100 nM. Plot of $\log(K_{app})$ against the estimated free cAMP concentrations are represented as filled symbols in Figure 3 (left panel). Careful examination of the fitted curve shows that the observed data are systematically lower than the fitted curve between 10 and 150 nM cAMP. This deviation is resulted from the uncertainty of the free cAMP concentration, as indicated by the filled symbols. Even though the total cAMP concentration did not reflect the free cAMP concentration in the range of 0−1 μM, the estimation of K_{11} and K_{12} was not affected by cAMP concentration in this case. All the fitting parameters are summarized in Table 2.

Validity of K_5 for lac−D53H CRP Interaction. Analysis of the amplitudes of the DNA binding isotherms provides an additional test of the validity of the determined parameter for cAMP binding to the DNA−CRP complex. The maximum change in anisotropy, ΔA, at each cAMP concentration is a measurement of the amount of cAMP−CRP−DNA

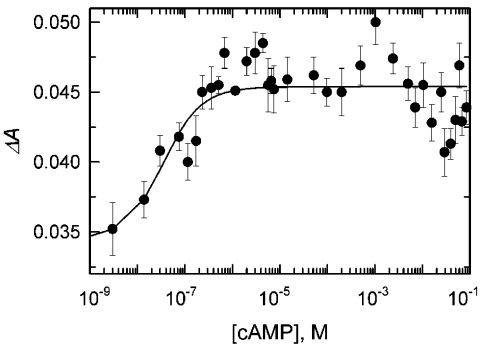

FIGURE 4: Dependence of the anisotropy change for the binding of D53H CRP to *lac26* on cAMP concentration. The error bars represent the standard deviation of the ΔA at each cAMP concentration. The solid line represents the simulation curve based on eq 3 with the values of $\Delta A_0 = 0.035$, $\Delta A_f = 0.045$, and $K_5 = 3.5 \times 10^7$ M^{-1}.

Table 3: Association Constant of cAMP Binding to D53H CRP−DNA Binary Complex

	lac26[a]	*gal26*
ΔA_0	0.035	0.032 ± 0.001
ΔA_f	0.045	0.063 ± 0.005
K_5	3.5×10^7 M^{-1} [b]	$(2.3 \pm 0.01) \times 10^7$ M^{-1}

[a] Parameters used for performing simulation. [b] Calculated value in accordance to $K_5 = K_1K_{10}/K_9$ (Table 2, case 4).

complex under these experimental conditions. Thus, a plot of ΔA versus cAMP concentration, as shown in Figure 4, should reflect the binding isotherm of cAMP to the CRP−DNA complex, of which the equilibrium constant is K_5 in accordance to Scheme 1. The data could be described by

$$\Delta A = \Delta A_0 + (\Delta A_f - \Delta A_0)\frac{K_5{\cdot}(DP_T + L_T) + 1 - \sqrt{(K_5{\cdot}(DP_T + L_T) + 1)^2 - 4(K_5)^2{\cdot}DP_T{\cdot}L_T}}{2K_5{\cdot}DP_T} \quad (3)$$

where L_T and DP_T are the total concentration of cAMP and DNA−CRP complex, respectively; ΔA is the fitting result of the anisotropy change according to eq 1 to the observed data as shown in Figure 1; ΔA_0 is the anisotropy change in the absence of cAMP; and ΔA_f is the anisotropy change at saturated level of cAMP. The error of ΔA_0 is relatively large for D53H CRP interacting with *lac26*, being limited by the smallness in change of amplitude. Nevertheless, on the basis of eq 3 and the values of $\Delta A_0 = 0.035$, $\Delta A_f = 0.045$, and $K_5 = 3.5 \times 10^7$ M^{-1} (Table 3), the simulation curve describes the observed data well, as shown in Figure 4, and validates the value of K_5 that was calculated through thermodynamic linkage.

gal26 Binding Affinity of D53H CRP Conformers. It is important to test the effect of DNA sequence on the behavior of D53H CRP conformers within the context of Scheme 1. The binding of D53H CRP to *gal26* at different concentrations of cAMP was conducted, and the results are shown in Figure 5A. When the data were analyzed with the same constraints as in case 4 for *lac26*, the result is shown as a dashed line in Figure 5A. Similar to the result for *lac26*, the fitted curve deviated systematically from the observed data at cAMP concentrations around 10^{-7} M. The various binding constants are summarized in Table 4. The basic pattern of

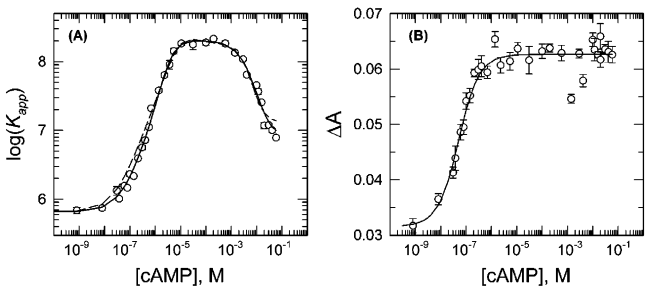

FIGURE 5: Dependence of the (A) apparent association constant (K_{app}) and (B) total anisotropy change (ΔA) for the binding of D53H to *gal26* on cAMP concentration. The error bars represent the standard deviation of the K_{app} and ΔA at each cAMP concentration. The solid lines represent the best fit of observed data according to eq 2 with the value of K_9 set at 6.5×10^5 M^{-1} and eq 3, respectively. The dashed line in panel A is the best fit of eq 2 to the observed data with K_1, K_2, and K_9 set at 4.1×10^4, 2.7×10^5, and 6.5×10^5 M^{-1}, respectively. The recovered parameters are listed in Tables 3 and 4.

behavior remains the same regardless of DNA sequence, namely, both PL and PL_2 conformers exhibit higher affinity for specific DNA sequence than PL_3. If K_1 and K_2 were set as variables to perform the fitting routine, the fit was improved with the result shown as the solid line in Figure 5A. The value of K_5 was experimentally determined by fitting the observed data to eq 3. The result is shown in Figure 5B. The fitted parameters are summarized in Table 3. The calculated (K_5 in Table 4) and experimental values are consistent with each other, and they are approximately 500-fold higher than K_1, the cAMP binding constant to CRP alone. Thus, the presence of DNA in the protein−DNA complex enhances significantly the affinity of CRP for cAMP.

lac40 Binding Affinity of D53H CRP Conformers in the Presence of cGMP. The interaction of cAMP with CRP at the high-affinity sites is characterized by cooperativity, although the magnitude and nature of cooperativity can be modulated by mutations (*22*). However, evidence supports noncooperative binding of cGMP to CRP (*22*). Therefore, it is of interest to define the pattern of D53H−DNA formation as a function of cGMP. The value of K_{app} governing the D53H−DNA formation is independent of the concentration of cGMP in the range of 0 nM to 20 mM. However, the apparent equilibrium constants for D53H−*lac26* complexes and its dependence on cAMP concentration exhibit a bell-shape relation, as shown in Figure 6.

DISCUSSION

Differential DNA Binding Affinity of CRP Conformers. A stoichiometry of four cAMP binding to CRP dictates that one must consider the possibility of five different DNA binding affinities for the five conformers, namely, P, PL, PL_2, PL_3, and PL_4 as shown in Scheme 1. On the basis of the results of linkage analysis summarized in Tables 2 (case 4) and 4 (case 1), the D53H CRP conformers that exhibit strong affinities to specific DNA sequences are the PL and PL_2, regardless of DNA sequence. Loading of the weak cAMP binding sites leads to a weaker affinity for DNA. The rank order of affinity is PL $\geq$ PL_2 > PL_3. This is the basis for the bell-shaped dependence on cAMP concentration of CRP−DNA complex formation, an observation that persists

Table 4: Summary of the Association Constants for the Formation of *gal26*−CRP−cAMP Tertiary Complex

case	constraints	recovered parameters	calculated parameters	
	$K_1 = 4 \times 10^4\ M^{-1}$	$K_3 = 103 \pm 128\ M^{-1}$	$K_5 = 3.8 \times 10^7\ M^{-1}$	$R^2 = 0.988$[a]
	$K_2 = 3 \times 10^5\ M^{-1}$	$n = 7 \pm 10$	$K_6 = 8.6 \times 10^4\ M^{-1}$	DW = 1.923[b]
1	$K_9 = 6.5 \times 10^5\ M^{-1}$	$K_{10} = (6.0 \pm 0.5) \times 10^8\ M^{-1}$	$K_7 = 7.6\ M^{-1}$	
	$K_4 = n^*K_3$	$K_{11} = (1.9 \pm 0.1) \times 10^8\ M^{-1}$	$K_8 = 731\ M^{-1}$	
	$K_{13} = K_{12}$	$K_{12} = (1.4 \pm 0.6) \times 10^7\ M^{-1}$		
	$K_9 = 6.5 \times 10^5\ M^{-1}$	$K_1 = (7 \pm 8) \times 10^4\ M^{-1}$	$K_5 = 2.1 \times 10^7\ M^{-1}$	$R^2 = 0.987$[a]
	$K_4 = n^*K_3$	$K_2 = (8 \pm 0.4) \times 10^5\ M^{-1}$	$K_6 = 8.0 \times 10^5\ M^{-1}$	DW = 2.28[b]
	$K_{13} = K_{12}$	$K_3 = (300 \pm 80)\ M^{-1}$	$K_7 = 11\ M^{-1}$	
2		$n = 0.5 \pm 0.6$	$K_8 = 130\ M^{-1}$	
		$K_{10} = (2.1 \pm 0.4) \times 10^8\ M^{-1}$		
		$K_{11} = (2.1 \pm 0.1) \times 10^8\ M^{-1}$		
		$K_{12} = (9 \pm 6) \times 10^6\ M^{-1}$		

[a] Adjusted R^2. [b] Durbin−Watson statistic.

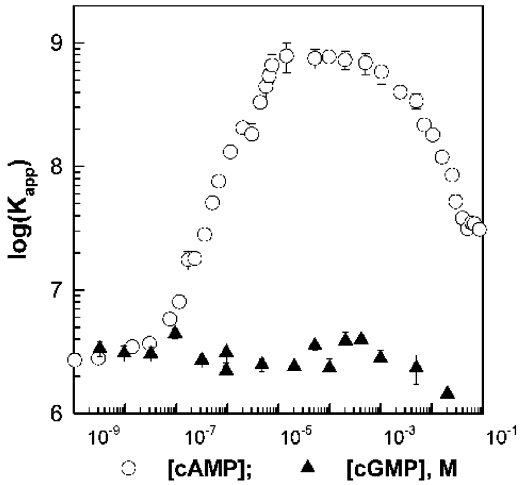

FIGURE 6: Plot of the log(K_{app}) against cGMP concentration for the formation of the D53H CRP−*lac40* complex. The K_{app} governing the D53H−*lac40* formation is independent of the concentration of cGMP (▲). The error bars represent the standard deviations obtained from the best fit of eq 1 to the DNA binding isotherms. For comparison, the K_{app} for the D53H−*lac26* formation as a function of cAMP concentration is plotted as an unfilled circle.

in all circumstances, be it WT or mutant CRP (*21*, *33*). Although both the PL and the PL_2 conformers show high affinity for DNA sequences, there is a difference between *lac26* and *gal26*. All the corresponding association constants for protein−DNA complex formation are higher for *lac26* than for *gal26*. This observation is consistent with the results from earlier studies that showed a higher affinity of cAMP−CRP for *lac26* than *gal26* (*21*, *31*, *33*).

The various association constants defined by this careful dissection of the linked reactions should at least be acceptable as to reflect the relative magnitude of these parameters. This conclusion is supported by the fact that the calculated value of K_5 is essentially identical to that measured directly. Furthermore, in the analysis of the data set for *gal26* (Table 4, case 2) when all parameters, with the exception of K_9, were left floating as fitting parameters, the recovered parameters assumed values of the same magnitude as those with additional constraints.

Apo-D53H CRP binds *lac26* with a binding constant of $2.4 \times 10^6\ M^{-1}$, which is an affinity that can be measured reasonably well with the in vitro technique, unlike that of the WT CRP that binds with a low value estimated to be $0.01 \times 10^6\ M^{-1}$, an affinity that is barely detectable with the fluorescence anisotropy technique. Thus, apparently a D53H mutation enhances the ability of CRP to bind to DNA.

It has been reported that protein dynamics is strongly related to protein function (*35*). For example, single mutant A77V of *trp* repressor stabilizes the helix-turn-helix domain and acts as super-repressor without increasing the DNA binding affinity (*36*). Recently, on the basis of the results of hydrogen−deuterium exchange, Dong et al. reported that the protein dynamics of the DNA binding domain in CRP increases upon cAMP binding (*23*). In contrast, cGMP does not induce a similar relaxation effect on the DNA binding domain. In addition, the cooperative binding of the two cAMP molecules to CRP at the high-affinity sites is driven by large positive entropy changes.[2] These observations support the contention that protein dynamics plays a key role in modulating the specific DNA sequence recognition. Although Asp 53 is located neither at the cyclic binding pocket nor at the DNA binding domain, it significantly affects the selectivity for ligand and the specificity for DNA. D53H exerts long-range effect for the function of CRP. Therefore, the changes in this protein may be related to protein dynamics. Detail experiments to test this hypothesis are currently in progress.

A linear correlation was established between the energetics of cooperativity in ligand interaction and that of the DNA binding, based on the study of WT and eight CRP mutants (*22*). It suggests that intersubunit communication upon cAMP binding confers in CRP the capability for DNA recognition. A D→H mutation enhances the cooperativity of cAMP binding and consequently increases DNA binding affinity, a 15-fold enhancement in *lac26* binding affinity as compared to that of the WT (Table 1). cGMP binds to D53H CRP in a noncooperative manner. Thus, cGMP apparently is unable to induce an intersubunit communication (*22*). Consequently, cGMP is unable to enhance the DNA binding affinity. This interpretation is supported by the observation that the apparent equilibrium constants for D53H−*lac40* complexes are independent of the concentrations of cGMP, as shown in Figure 6. Another linear correlation was established between the ability to discriminate between cNMP and the energetics of subunit assembly (*21*). The greater ability to discriminate between cNMP is correlated with stronger subunit interaction. The energetics of D53H CRP subunit interaction is similar to that of WT CRP (*21*). Thus, the distinctive difference in response to cAMP and cGMP by D53H CRP can be expected.

[2] Lin, S.-H. and Lee, J. C., manuscript in preparation.

Table 5: Free Energy Changes in DNA−CRP Interactions

CRP	DNA	$-\Delta G$ (kcal/mol)	$-\Delta\Delta G$ (kcal/mol)
WT[a,b]	NS[c]	6.3	
	gal	9.5	3.2
	lac	10.3	4.0
D53H[b]	NS	7.8	
	gal	11.3	3.5
	lac	12.7	4.9
D53H[d]	NS	6.2	
	gal	7.9	1.7
	lac	8.7	2.5

[a] Data from ref *31*. [b] In the presence to 200 μM cAMP. [c] Nonspecific. [d] In the absence of cNMP.

Relevance to WT CRP. How relevant are the results of the D53H CRP in revealing the mechanism of WT CRP? These results are relevant since the mutation does not alter the basis mechanism of CRP activation but merely shifted the various thermodynamically linked reactions to a regime that is more amenable to the in vitro measurements for precise quantitation. Let's examine the evidence that supports this conclusion. In cAMP binding, both WT and D53H CRP exhibit the presence of two sets of two binding sites (*22*). There is positive cooperativity between the two high-affinity binding sites, although the D53H mutation evidently enhances this interaction between sites. The low-affinity binding sites can be best described to exhibit negative cooperativity. In DNA recognition, both WT and D53H CRP bind to specific DNA sequences with high affinity when the high-affinity sites are occupied, while the occupancy of the weak cAMP sites leads to substantially weaker affinity for DNA (*22*). Furthermore, the rank order of affinity for various DNA sequences is the same, as summarized in Table 1. The rank order of increasing affinity for WT CRP is *nonspecific*, *gal26*, and *lac26*, the same order as for D53H CRP. Interestingly, the magnitude of $\Delta\Delta G$, the difference in the energetics of binding to different DNA sequences, is quite similar (Table 5). Hence, these results support the proposal that the D53H mutation merely shifts all the DNA binding constants to higher values without altering the mechanism of recognition.

How does the mutation shift these binding constants without altering the basic mechanism? One possibility is through a perturbation of the distribution of the ensemble of CRP structures. Recently, Pan et al. (*37*) showed that the ensemble theory could capture the basic features of allosteric behavior of *E. coli* dihydrofolate reductase including the effects of mutations. A detailed study is in progress to address this particular issue.

Biological Significance. The binding constant of cAMP to the high-affinity sites in CRP is about 30−40 μM (Tables 1 and 2 in ref 22). However, in vivo studies indicate that cAMP−CRP-dependent operons are responsive to a cAMP concentration regime that is significantly lower (*38*). To resolve this apparent inconsistency between the in vivo and the in vitro results, it is important to focus on the value of K_5 (i.e., the binding constant of cAMP to the DNA−CRP complex) (Scheme 1 and Tables 2−4). The values of K_5 are 900 and 400-fold greater than the corresponding binding constant to apo-CRP, K_1, in *lac26* and *gal26*, respectively (i.e., K_5 assumes the value of $2-4 \times 10^7$ M^{-1}). This high affinity for cAMP for the CRP−DNA complex places the regime of cAMP concentration at which it responses in the same one as in the in vivo study (*38*). In vivo, K_5 is the relevant binding constant because the concentration of CRP has been estimated to be 2.5 μM in the cell (*39*). At such a high CRP concentration, significant amount of CRP will be complexed with DNA in the absence of cAMP. Thus, cAMP will be binding to the DNA−CRP complex even with an intracellular concentration fluctuation of less than μM of cAMP, a mechanism proposed by Takahashi et al. (*40*). A simulation on the change in the DNA−CRP−cAMP complex as a function of CRP and cAMP concentrations is shown in Figure 7. It is evident that at the physiological concentration of CRP (>1 μM), the amount of DNA−CRP−cAMP complex fluctuates most significantly at cAMP concentration below 1 μM. Figure 7 also illustrates the effect of a decrease in intercellular CRP concentration. Not only a smaller amount of DNA−CRP−cAMP complex is formed, but also the effective cAMP concentration is extended to a much higher concentration regime.

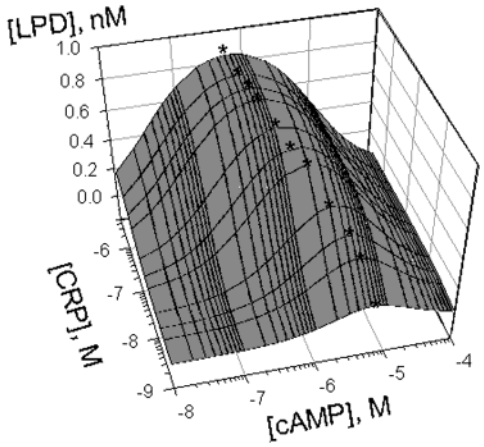

FIGURE 7: Distribution of CRP−DNA−cAMP ternary complex as a function of cAMP and CRP concentrations. Simulation is based on the model shown in Scheme 1, using parameters listed in Table 2, and $[DNA]_{total} = 1$ nM. The asterisk indicates the cAMP concentration at which the maximum amount of the ternary complex is present.

Having established the relevance of K_5 and that probably the intracellular concentration of the DNA−CRP complex is significant, let us examine the significance of K_6, the binding constant of the second cAMP to the DNA−CRP complex. For *lac26*, K_6 is approximately 350-fold weaker than K_5, and if expressed in terms of dissociation constant then it is about 10 μM. If the intracellular concentration of cAMP fluctuates around 1−2 μM, then the predominant species would be *lac*−CRP−cAMP and not *lac*−CRP−$cAMP_2$. A homodimeric CRP with one cAMP bound is structurally asymmetric. This raises the issue of the significance of an asymmetric CRP−cAMP complex binding to a DNA sequence that is asymmetric also. However, for *gal26*, K_6 is only approximately 30-fold weaker than K_5 and is about 1 μM when expressed as a dissociation constant. It is conceivable that a significant amount of the ternary complex exists as a mixture of *gal*−CRP−cAMP and *gal*−CRP−$cAMP_2$ (e.g., approximately 60:40 distribution at 1 μM of cAMP). The biological rationale for the difference in the DNA recognition pattern of the two conformers in these promoters needs to be investigated.

CONCLUDING REMARKS

Only through a dissection of the thermodynamic linkages of CRP−cAMP−DNA interactions that it becomes possible to identify the mechanism through which CRP functions in the cell. In addition, these results provide a rationale to explore the potential biological significance of the singly liganded species of cAMP−CRP−DNA.

REFERENCES

1. Aiba, H., Fujimoto, S., and Ozaki, N. (1982) *Nucleic Acid Res. 10*, 1345−1361.
2. Cossart, P., and Gicquel-Sanzey, B. (1982) *Nucleic Acid Res. 10*, 1363−1378.
3. Weber, I. T., and Steitz, T. A. (1987) *J. Mol. Biol. 198*, 311−326.
4. Krakow, J. S., and Pastan, I. (1973) *Proc. Natl. Acad. Sci. U.S.A. 70*, 2529−2533.
5. Wu, F. Y. M., Nath, K., and Wu, C.-W. (1974) *Biochemistry 13*, 2567−2572.
6. Wu, C.-W., and Wu, F. Y. H. (1974) *Biochemistry 13*, 2573−2578.
7. Eilen, E., and Krakow, J. S. (1977) *J. Mol. Biol. 114*, 47−60.
8. Pampeno, C., and Krakow, J. S. (1979) *Biochemistry 18*, 1519−1525.
9. Lee, B. J., Lee, S. J., Hayashi, F., Aiba, H., and Kyogoku, Y. (1990) *J. Biochem. 107*, 304−309.
10. Sixl, F., King, R. W., Bracken, M., and Feeney, J. (1990) *Biochem. J. 266*, 545−552.
11. Hinds, M. G., King, R. W., and Feeney, J. (1992) *Biochem. J. 287*, 627−632.
12. Gronenborn, A. M., and Clore, G. M. (1982) *Biochemistry 21*, 4040−4048.
13. Tan, G. S., Kelly, P., Kim, J., and Wartell, R. M. (1991) *Biochemistry 30*, 5076−5080.
14. McKay, D. B., Weber, I. T., and Steitz, T. A. (1982) *J. Biol. Chem. 257*, 9518−9524.
15. Schultz, S. C., Shields, G. C., and Steitz, T. A. (1991) *Science 253*, 1001−1007.
16. Passner, J. M., Schultz, S. C., and Steitz, T. A. (2000) *J. Mol. Biol. 304*, 847−859.
17. Cheng, X. D., Kovac, L., and Lee, J. C. (1995) *Biochemistry 34*, 10816−10826.
18. Cheng, X. D., and Lee, J. C. (1998) *Biochemistry 37*, 51−60.
19. Cheng, X. D., and Lee, J. C. (1998) *J. Biol. Chem. 273*, 705−712.
20. Shi, Y., Wang, S., Krueger, S., and Schwarz, F. P. (1999) *J. Biol. Chem. 274*, 6946−6956.
21. Lin, S.-H., Kovac, L., Chin, A. J., Chin, C. C. Q., and Lee, J. C. (2002) *Biochemistry 41*, 2946−2955.
22. Lin, S.-H., and Lee, J. C. (2002) *Biochemistry 41*, 11857−11867.
23. Dong, A., Malecki, J., Lee, L., Carpenter, J. F., and Lee, J. C. (2002) *Biochemistry 41*, 6660−6667.
24. Heyduk, E., Heyduk, T., and Lee, J. C. (1992) *Biochemistry 31*, 3682−3688.
25. Heyduk, T., and Lee, J. C. (1989) *Biochemistry 28*, 6914−6924.
26. Sanders, R., and McGeoch, D. (1973) *Proc. Natl. Acad. Sci. U.S.A. 70*, 1017−1021.
27. Dessein, A., Schwartz, M., and Ullmann, A. (1978) *Mol. Gen. Genet. 162*, 83−87.
28. Kim, J., Adhya, S., and Garges, S. (1992) *Proc. Natl. Acad. Sci. U.S.A. 89*, 9700−9704.
29. Takahashi, M., Blazy, B., and Baudras, A. (1980) *Biochemistry 19*, 5124−5130.
30. Merck & Co., Inc. (1976) in *Merck Index*, 9th ed., p 353, Rahway, NJ.
31. Pyles, E. A., Chin, A. J., and Lee, J. C. (1998) *Biochemistry 37*, 5194−5200.
32. Heyduk, T., and Lee, J. C. (1990) *Proc. Natl. Acad. Sci. U.S.A. 87*, 1744−1748.
33. Pyles, E. A., and Lee, J. C. (1996) *Biochemistry 35*, 1162−1172.
34. Cheng, X. D., and Lee, J. C. (1994) *J. Biol. Chem. 269*, 30781−30784.
35. Stock, A. (1999) *Nature 400*, 221−222.
36. Gryk, M. R., and Jardetzky, O. (1996) *J. Mol. Biol. 255*, 204−214.
37. Pan, H., Lee, J. C., and Hilser, V. J. (2001) *Proc. Natl. Acad. Sci. U.S.A. 97*, 12020−12025.
38. Lis, J. T., and Schleif, R. (1973) *J. Mol. Biol. 79*, 149−162.
39. Zubay, G. (1980) *Methods Enzymol. 65*, 856−877.
40. Takahashi, M., Blazy, B., Baudras, A., and Hillen, W. (1989) *J. Mol. Biol. 207*, 783−796.

BI026756N